

Communication at the quantum speed limit along a spin chain

Michael Murphy* and Simone Montangero

Institut für Quanteninformationsverarbeitung, Universität Ulm, Albert-Einstein-Allee 11, D-89069 Ulm, Germany

Vittorio Giovannetti

National Enterprise for nanoScience and nanoTechnology–Consiglio Nazionale delle Ricerche–Istituto Nazionale per la Fisica della Materia & Scuola Normale Superiore, P.zza dei Cavalieri 7, D-56126 Pisa, Italy

Tommaso Calarco

Institut für Quanteninformationsverarbeitung, Universität Ulm, Albert-Einstein-Allee 11, D-89069 Ulm, Germany

(Received 20 April 2010; published 13 August 2010)

Spin chains have long been considered as candidates for quantum channels to facilitate quantum communication. We consider the transfer of a single excitation along a spin-1/2 chain governed by Heisenberg-type interactions. We build on the work of Balachandran and Gong [V. Balachandran and J. Gong, *Phys. Rev. A* **77**, 012303 (2008)] and show that by applying optimal control to an external parabolic magnetic field, one can drastically increase the propagation rate by two orders of magnitude. In particular, we show that the theoretical maximum propagation rate can be reached, where the propagation of the excitation takes the form of a dispersed wave. We conclude that optimal control is not only a useful tool for experimental application, but also for theoretical inquiry into the physical limits and dynamics of many-body quantum systems.

DOI: [10.1103/PhysRevA.82.022318](https://doi.org/10.1103/PhysRevA.82.022318)

PACS number(s): 03.67.Hk, 03.67.Lx, 75.10.Pq, 78.67.Lt

I. INTRODUCTION

Quantum computers promise to allow efficient simulation of large dynamic and complex systems and deliver performance advantages over their classical counterparts. One of the central considerations for the construction of a quantum computer is an infrastructure that can rapidly and robustly transport qubit states between sites where qubit operations can be performed. The components for this infrastructure may be thought of as quantum channels for quantum information transfer. One of the technologies under investigation to constitute such a channel is the one-dimensional spin chain [1–10], which consists of a string of particles coupled via their spin degrees of freedom, each acting as an effective two-level quantum system. As is customary in quantum information processing, proper engineering of the control parameters of the system is essential to achieve the high fidelity necessary for robust quantum computation. This can be obtained, for instance, by employing a numerical optimization method which, for the specific settings of the problem, seeks the optimal control pulses that allow one to implement the desired operation [11–21]. In this paper, we apply such a method, known in the literature as the Krotov method [22,23], to the case of quantum state transfer along a one-dimensional spin chain. The specific system we use was introduced by Balachandran and Gong [1], but here we show that by designing the external driving parameters with optimal control methods, one can obtain a significant increase in fidelity, even over short timescales [24].

These high-fidelity, high-speed transmissions exhibit interesting characteristics. If one ignores the effects taking place near the boundaries of the chain, the evolution of the excitation

is that of a dispersed wave, moving with almost constant velocity along the chain. This velocity is independent of the chain length, and furthermore has an upper bound, indicating the presence of a fundamental limit on the rate of transmission. Through a closer analysis, we show that this limit can be directly related to the theoretical maximum speed of the state transfer allowable by the laws of quantum mechanics [25–29].

Producing time-optimal gates has already been explored in the literature [30–34] where the authors considered geodesics on the Bloch sphere for systems with a low number of dimensions. Unfortunately, extension of these methods to many-body systems (such as the system we consider here) are prohibitively difficult. Conversely, the numerical optimization methods that we employ have little difficulty in finding sets of optimal solutions, even at this limit. In effect, we demonstrate that through application of optimal control, we cannot only transmit the excitation with a high fidelity, but also at the fastest possible speed. One can even reverse the problem, implying that optimal control can be used to probe such fundamental dynamical limits on many-body quantum systems. Such tools will be invaluable as the ambition of quantum science leads it toward investigations of systems of greater complexity which are less tractable analytically.

The paper is arranged as follows. In Sec. II, we describe the system used for information transfer in more detail and the precise scheme which we will use for propagating quantum information in the system. Section III discusses the application of optimal control to the transfer scheme, and shows that optimal control can effect significant gains in the transfer speed. We then discuss the fundamental limit of these improvements in Sec. IV, and show that optimal control in fact allows us to reach this limit, thus allowing us to transfer the spin state in the fastest possible time allowable by the laws of quantum mechanics. Finally, we present the conclusions in Sec. V.

*michael.murphy@uni-ulm.de

II. SPIN CHAINS AS QUANTUM CHANNELS

A. Overview

Using spin chains as quantum channels for communication between two parties was first proposed by Bose in 2003 [6] and later developed in a series of papers (we refer the reader to Ref. [2] for a review). The idea is relatively simple: Alice (the sender) has a quantum state she wants to relay to Bob (the receiver). Between them is a one-dimensional chain of N spin-1/2 particles which are coupled via nearest-neighbor interactions. Alice has access to the first spin in this chain, and can prepare its spin state as she chooses. Bob has access to the final site (the terms “spin” and “site” will be used interchangeably), whose state he can read out. Following [1], we apply an external parabolic magnetic field, which Alice can control. The procedure for sending quantum information along the chain is as follows.

- (1) The spin chain is prepared in its ground state with respect to the external magnetic field.
- (2) Alice prepares the initial spin state to be the state she wishes to transfer.
- (3) By manipulating the magnetic field, Alice controls the propagation of the spin along the chain, which takes place due to the coupling between the spin degrees of freedom.
- (4) After some prescribed time when the state has been transferred to the final site, Bob reads out the state of this site.

B. The Hilbert space and Hamiltonian

The model we consider is sketched in Fig. 1. It is composed of a one-dimensional spin-1/2 chain with N sites, where distances are measured by the variable x (although this may not be a physical distance). We will consider uniform Heisenberg nearest-neighbor couplings characterized by the same coupling strength J , and the presence of a parabolic external magnetic field in the z direction, normal to the direction x . Consequently, the field will act on the n th site as

$$B_n(t) = C(t)[x_n - d(t)]^2, \quad (1)$$

where $d(t)$ is the position of the field minimum along x at time t , and $C(t)$ is a measure of the global field strength.

The Hamiltonian then takes the form,

$$H(t) = -\frac{J}{2} \sum_{n=1}^{N-1} \vec{\sigma}_n \cdot \vec{\sigma}_{n+1} + \sum_{n=1}^N B_n(t) \sigma_n^z, \quad (2)$$

where n labels the spin sites, with $n = 1$ and $n = N$ referring to the first and last spins, respectively, and $\vec{\sigma}_n = (\sigma_n^x, \sigma_n^y, \sigma_n^z)$ are the Pauli spin operators for the n th spin. For convenience,

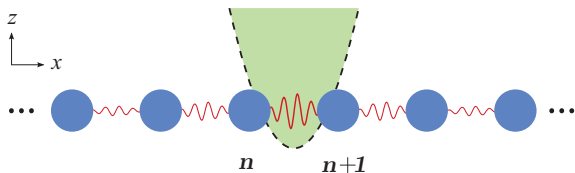


FIG. 1. (Color online) The one-dimensional spin chain used for information transfer. The (blue) solid circles represent sites along the chain, with the applied magnetic field depicted. The effective couplings are indicated operating between the sites.

all system parameters are scaled to make them dimensionless, and the coupling strength is set to $J = 1$.

The dynamics are governed by the interplay between the nearest-neighbor interactions and the interaction of each site with the external parabolic magnetic field. When sites are far from the field minimum, the local field strength dominates over the nearest-neighbor interactions, effectively “switching off” the coupling between sites. For sites near the minimum where the field is weak, the nearest-neighbor coupling dominates, and the neighboring sites interact with each other. These two processes control the propagation of spin states along the chain.

C. Communicating quantum information

We identify the computational basis for our system with the quantized states of each spin, such that $|0\rangle = |\downarrow\rangle$ (spin down with respect to z) and $|1\rangle = |\uparrow\rangle$ (spin up). Assume that Alice prepares the chain in the initial state $|\Psi(0)\rangle$, with the first spin site in the state $|1\rangle$, and all other sites in their ground state $|0\rangle$. We can write this state as

$$|\Psi(t=0)\rangle = |\varphi_1\rangle \equiv |1\rangle \otimes |0\rangle \otimes |0\rangle \otimes \cdots \otimes |0\rangle, \quad (3)$$

with the first spin site in the state $|1\rangle$, and all other sites in their ground state $|0\rangle$. The states $|\varphi_n\rangle$ are defined as

$$|\varphi_n\rangle \equiv \bigotimes_{m=1}^N |\delta_{mn}\rangle, \quad n = 1, \dots, N, \quad (4)$$

where δ_{mn} is the Kronecker delta. Alice’s goal is to manipulate the magnetic field parameters $C(t)$ and $d(t)$ such that at the final time T the final state obeys

$$|\langle \Psi(T) | \varphi_N \rangle|^2 = 1. \quad (5)$$

The protocol for transferring the state is based on that described in Ref. [1], which we outline in Fig. 2. The transfer begins with the state $|\Psi(0)\rangle$ and with the potential minimum centered at $x = 0$. At first, the interaction between the first two sites

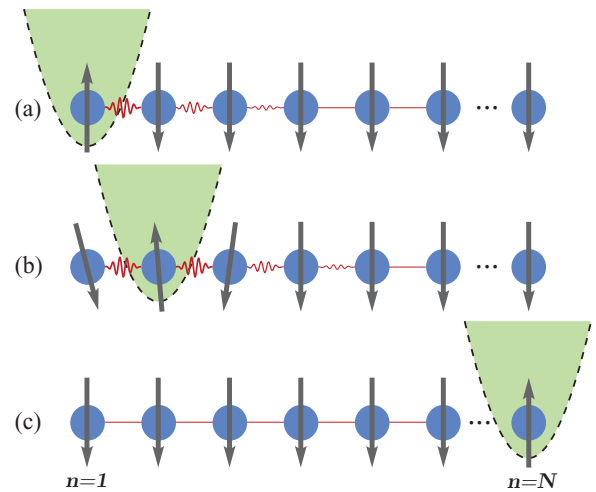


FIG. 2. (Color online) The transfer begins with the state $|\Psi(0)\rangle$ and with the potential minimum centered at $x = 0$. (a) The excitation is localized at the first site. (b) The field minimum moves along the chain during the evolution. (c) The spin state has been completely transferred to the final site in the chain.

dominates over the interaction with the locally weak magnetic field, and so the sites interact and the spin state migrates from the first site to the second. As the field minimum moves along the x axis, nearest-neighbor interactions are effectively switched on for pairs of spins closest to the minimum, and switched off for spin pairs that are distant. By correctly moving the field minimum and adjusting the field strength, the spin state is able to traverse the chain. The condition in Eq. (5) means that we do not preserve the phase of the initial state; to achieve this (as also discussed in Ref. [1]) one can use dual-rail encoding [35–37], whereby one encodes the qubit in the entanglement phase of a pair of spin chains. In what follows, we shall only consider the phase-insensitive transfer of a single excitation.

Since each site of the chain has two internal spin states, the size of the Hilbert space \mathcal{H} scales exponentially with the number of sites, so that for $N(\geq 1)$ sites, $\dim \mathcal{H} = 2^N$. However, since $[H(t), \sum_{n=1}^N \sigma_n^z] = 0$, the state of the system only evolves within the subspace $\mathcal{U} \subset \mathcal{H}$, spanned by the N basis states $|\phi_n\rangle$ [2]. The reduced size of the effective Hilbert space is particularly beneficial when one wants to numerically simulate the evolution efficiently. We do this by solving the associated Schrödinger equation,

$$i \frac{\partial}{\partial t} |\Psi(t)\rangle = \hat{H}(t) |\Psi(t)\rangle, \quad (6)$$

where \hat{H} is the matrix form of the Hamiltonian that acts only on the subspace \mathcal{U} ,

$$\hat{H}(t) \equiv \hat{H}_0 + \hat{H}_1(t), \quad (7)$$

with

$$\hat{H}_0 = -2J + J \begin{pmatrix} 1 & 1 & 0 & \cdots & 0 & 0 \\ 1 & 0 & 1 & & 0 & 0 \\ 0 & 1 & 0 & & 0 & 0 \\ \vdots & & & \ddots & & \vdots \\ 0 & 0 & 0 & & 0 & 1 \\ 0 & 0 & 0 & \cdots & 1 & 1 \end{pmatrix}, \quad (8)$$

and

$$\hat{H}_1(t) = \text{diag}[f_0(t), f_1(t), \dots, f_{N-1}(t)], \quad (9)$$

where $f_n(t) = C(t)[x_n - d(t)]$ (note that we have rescaled the energy so that spins pointing down do not contribute to the total energy). The Schrödinger equation is integrated numerically using the Crank-Nicolson method [38].

This scheme was first considered by Balachandran and Gong [1], who showed that by choosing $d(t) = st$ and $C(t) = k$, where s and k are constant, one is able to adiabatically transfer the state across the entire chain with relatively good fidelities. However, the transfer rates here are very slow, with transfer times typically on the order of $10^4 J$ for fidelities greater than 99%.

In many proposed implementations of quantum computers, it is likely that transport processes will take up a significant amount of the total operating time. It therefore seems clear that one should seek to minimize the time required for these processes. However, according to quantum mechanics there is some fundamental limit which restricts the speed at which we can communicate with our spin chain, referred to in the

literature as the quantum speed limit (QSL) [25–29,39]. The goal is to come as close as possible to this limit, effectively communicating at the highest possible speed allowable by quantum mechanics. We shall see in the next section that optimal control can help us in this endeavor.

III. OPTIMAL DYNAMICS

We can state our problem in the following way: we start with an initial state, and want to control the system to produce the desired final state. In our case, the initial state is $|\varphi_1\rangle$, and we want to achieve the final state $|\varphi_N\rangle$ (up to a global phase). We can control the evolution of the system using the external magnetic field, in particular, the time-dependent controls $d(t)$ and $C(t)$. (Although in principle we could also control the interspin coupling J , this is much more difficult to achieve experimentally.) Optimal control theory provides us with a set of tools to search for the optimal way to control the system, often referred to as the set of optimal *controls*.

Here, we implement an optimal control algorithm most commonly known as the Krotov method. In outline, the method works as follows.

(1) We solve the Schrödinger equation from (6) to find $|\Psi(T)\rangle$, where T is the total evolution time.

(2) We define the co-state $|\chi(T)\rangle = |\varphi_N\rangle \langle \varphi_N | \Psi(T)\rangle$. This state is propagated backwards to the initial time.

(3) The initial state is then propagated forward again through time, but at each time step we calculate the matrix elements,

$$\langle \chi(t) | \frac{\partial H(u_n(t); t)}{\partial u_n(t)} | \Psi(t) \rangle, \quad (10)$$

for the two controls $u_1(t) = d(t)$ and $u_2(t) = C(t)$. The matrix elements are then used to update the control functions, which are then used to propagate $\Psi(t)$ to the next time step.

(4) We can then calculate the fidelity of the transport,

$$F \equiv |\langle \Psi(T) | \varphi_N \rangle|^2, \quad (11)$$

which tells us how close we were to achieving our goal. (Note that we will often refer not to the fidelity, but to the infidelity $I \equiv 1 - F$.) If we achieve fidelity $F = 1$ (up to a given threshold), we stop the optimization; otherwise we begin again at step III.

There are several aspects in implementing the algorithm which are described in more detail in Ref. [22]. Figure 3 shows the nonadiabatic transfer of a spin excitation across a chain of $N = 101$ spins without applying optimal control. One sees that during propagation, much of the spin excitation has been left behind. One way to correct this would be to lower the field strength; this will allow neighboring sites to interact for longer, so that more of the excitation can be transmitted. However, this causes the excitation to spread out, which can be seen in Fig. 4. In comparison with Fig. 3, we see that although we have not left as much of the excitation behind, we have spread it over more sites. After applying optimal control (300 iterations of the update procedure), we arrive at the evolution shown in Fig. 5. Here we see that we no longer leave excitation behind at the initial spin sites, and although we spread out the excitation during transport, we successfully recover the highly localized final state, giving a final fidelity F that differs from

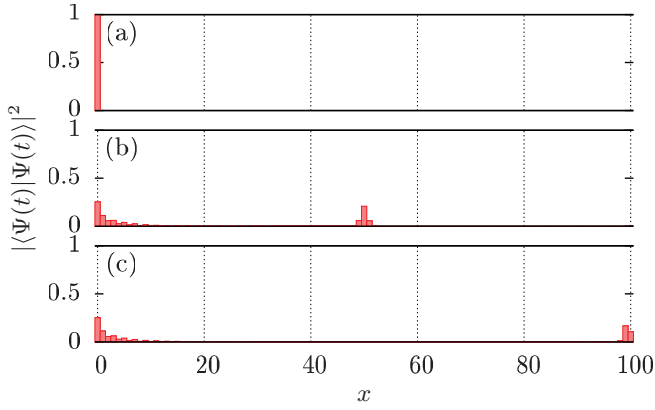


FIG. 3. (Color online) Excitation probability plotted against x for a spin chain with $N = 101$ sites, at times (a) 0, (b) 100, and (c) 200, in units of J^{-1} . Here, $d(t) = 0.5t$ and $C(t) = 1$. The final fidelity is only around 15%.

unity by $< 10^{-4}$. The pulses required to achieve this result are shown in Fig. 6. Typical features of these pulses are large modulations at the boundaries, necessary for “accelerating” (it will be useful here to imagine an excitation wave) the excitation at the initial time, and then “decelerating” it near the final time. Small modulations are required at intermediate times in order to prevent the excitation from spreading over too many sites. It is also worth noting that the speed achieved here is at least two orders of magnitude faster than is possible in the adiabatic case for comparable fidelities [1].

If we decrease T , we find for all times T shorter than a particular time T_{QSL}^* that even after applying the optimization algorithm we are still unable to achieve high-fidelity state transfer. In other words, there is a minimum time required to perform the transfer [29]. The lower bound on the value of T_{QSL}^* is set by the quantum speed limit; no transfer can take place faster than the QSL allows. Figure 7 shows the same transfer of excitation as in Fig. 5, but in this case we have set the total allowed time $T = T_{\text{QSL}}^*$ (how we determined T_{QSL}^* is shown later). One sees clearly that the evolution of the system is that of a wave of excitation, moving with an

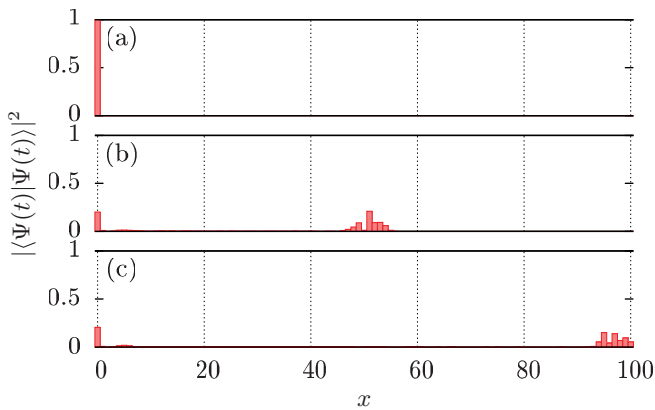


FIG. 4. (Color online) Excitation probability plotted against x for a spin chain with $N = 101$ sites, at times (a) 0, (b) 100, and (c) 200, in units of J^{-1} . Here, $d(t) = 0.5t$ and $C(t) = 0.1$. The final fidelity here is around 5%.

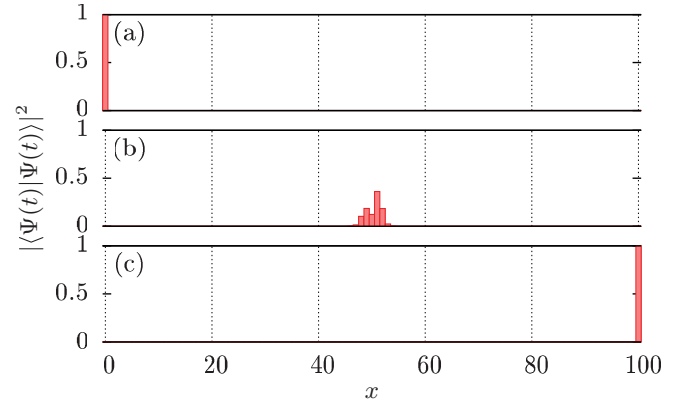


FIG. 5. (Color online) Excitation probability plotted against x for a spin chain with $N = 101$ sites, at times (a) 0, (b) 100, and (c) 200, in units of J^{-1} . Here, $d(t)$ and $C(t)$ were optimally controlled. The final fidelity is $>99\%$.

almost constant velocity along the chain. When we choose time $T < T_{\text{QSL}}^*$, we find accordingly that the optimal control algorithm is unable find an optimal solution, even after many thousands of iterations. This is a strong indication that we have gone beyond the quantum speed limit, and there is no solution by which we can transfer the excitation across the chain in the given time. The evolution of the system in this case is shown in Fig. 8. In comparison to Fig. 7, one sees that the evolution looks much the same. However, if one compares the excitation profile at $T/2$ for both evolutions, one sees that while the evolution at the QSL has the excitation wave centered at the 51st site (i.e., the halfway point), the evolution for a time $T < T_{\text{QSL}}^*$ falls short of the halfway point after $T/2$. This is an indication that we are indeed beyond the QSL, since if we cannot reach the halfway point before half the time has elapsed, we might well guess that we cannot reach the final site in the remaining half of the time.

We can see this failure of the optimization algorithm more clearly in Fig. 9. For times $T > T_{\text{QSL}}^*$, the infidelity converges almost exponentially toward zero. For times

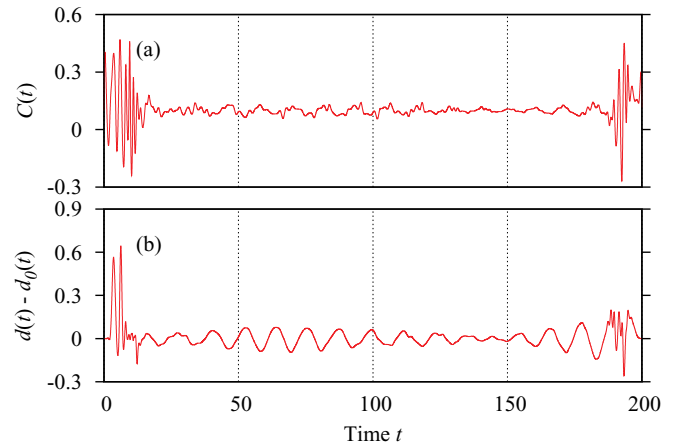


FIG. 6. (Color online) The optimal control pulses for (a) $C(t)$ and (b) $d(t) - d_0(t)$, where $d_0(t) = 0.5t$. The main features here are large perturbations at the initial and final time due to the boundaries, and slower modulations for the intermediate stage of the transport.

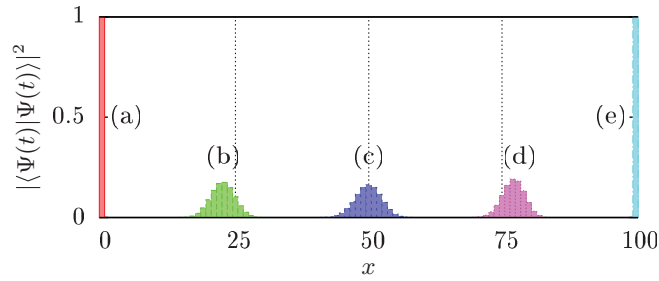


FIG. 7. (Color online) The probability density of the wave function along the chain at different times: (a) $t = 0$, (b) $t = T/4$, (c) $t = T/2$, (d) $t = 3T/4$, and (e) $t = T$, where $T = T_{\text{QSL}}^* = 56.50J^{-1}$. Both $d(t)$ and $C(t)$ were found after 100,000 iterations of the optimal control algorithm.

$T < T_{\text{QSL}}^*$, the decrease in infidelity saturates after several hundred iterations.

Another indication that the QSL has been reached can be found by examining the average “velocity” of the excitation wave as it moves across the chain. Given a total time T for the propagation, the average rate at which the excitation *should* be transmitted is given by $v_a = (N - 1)/T$. Examining the dynamics, we can see that for much of the propagation time, the excitation moves along the chain with an (approximately) constant velocity. We can quantify this velocity as

$$v_d = \frac{4}{T^2} \int_{T/4}^{3T/4} \langle x \rangle dt, \quad (12)$$

where $\langle x \rangle = \langle \Psi(t) | x | \Psi(t) \rangle$ is the expectation value of the position of the excitation along the chain. In other words, we take the average position of the excitation in the time interval $[T/4, 3T/4]$ (to avoid effects at the ends of the chain) and divide by the average time taken to reach that position, $T/2$.

In the ideal case, we would have $v_a = v_d$, in which case the optimal solution would be the transit of the excitation along the chain at exactly the average rate required to reach the other end. However, as we cross the threshold set by the QSL, we should find that v_d reaches a maximum, which is the maximum speed at which the excitation can propagate. This is exactly what is seen in Fig. 10.

The last issue we want to address is robustness. In essence, how much information in the control pulses given in Fig. 6 (and indeed in all of the control pulses at the QSL) can be

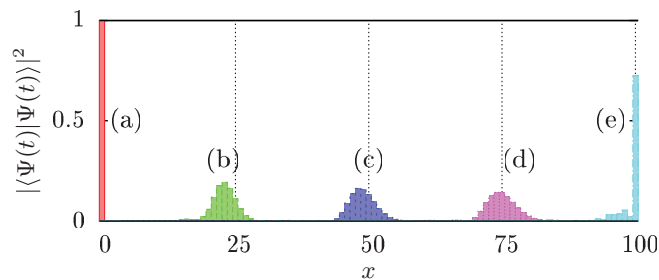


FIG. 8. (Color online) The probability density of the wave function along the chain at different times: (a) $t = 0$, (b) $t = T/4$, (c) $t = T/2$, (d) $t = 3T/4$, and (e) $t = T$, where $T < T_{\text{QSL}}^* = 53.30J^{-1}$. Both $d(t)$ and $C(t)$ were found after 100,000 iterations of the optimal control algorithm.

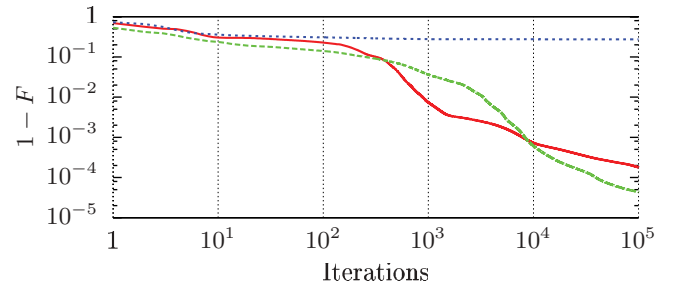


FIG. 9. (Color online) The decrease in infidelity of a transfer across a chain with 101 sites against the iterations of the control algorithm. The solid (red) line is the convergence for a transfer time $T = 70.92J^{-1} > T_{\text{QSL}}^*$, the dashed (green) line for a transfer time $T = T_{\text{QSL}}^* = 56.50J^{-1}$, and the dotted (blue) line for a transfer time of $T < T_{\text{QSL}}^* = 53.33J^{-1}$.

discarded without detriment to the transfer fidelity? Figure 11 shows an example spectrum of a pulse for $d(t)$ for a transfer along a chain of 101 spins at the QSL, and Fig. 12 shows the effect on the fidelity after filtering the optimized pulses. The filter applied is a simple frequency cutoff: the pulse (in frequency space) is convoluted with a function,

$$\gamma(v; v_{\text{max}}) = \begin{cases} v & \text{if } |v| \leq v_{\text{max}}, \\ 0 & \text{otherwise,} \end{cases} \quad (13)$$

where v_{max} is the maximum allowed frequency in the pulse. We see that not all of the frequencies in the control pulses need be retained; on average, we only need frequencies up to around $4J$ in order to maintain a high fidelity. Note that this is independent of the chain length N . Figure 13 shows a set of pulses that transport the excitation along a chain of 101 spins with an infidelity $I < 10^{-4}$, where the maximum frequency component is $\sim 4J$.

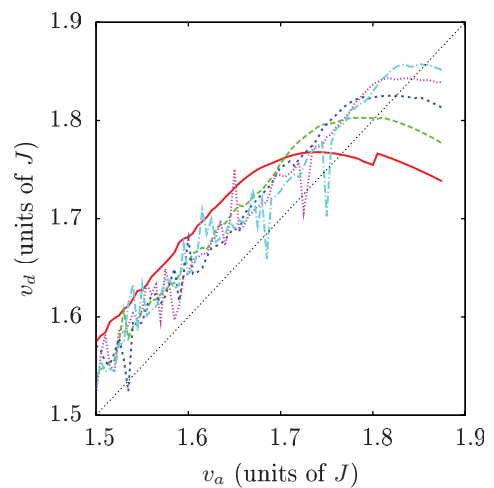


FIG. 10. (Color online) The average speed of the excitation wave v_d versus v_a . The solid (red) line shows results for a chain length of 41 sites, the long-dashed (green) line shows the same for 61 sites, the short-dashed (dark blue) line for 81 sites, the dotted (pink) line for 101 sites, and the dashed-dotted (light blue) line for 121 sites. The black dotted line is the line $v_a = v_d$.

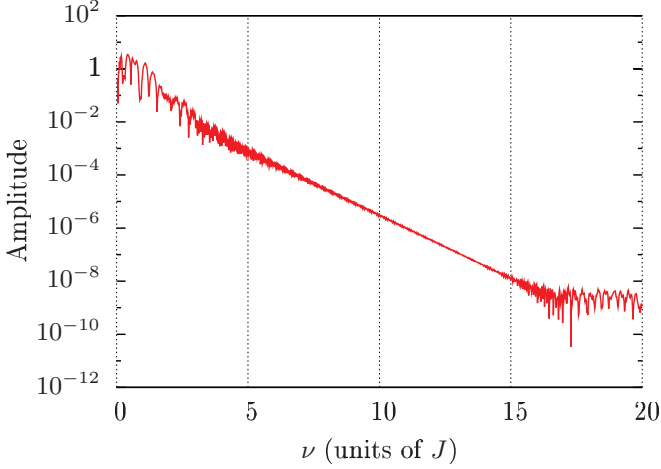


FIG. 11. (Color online) The solid (red) line shows the Fourier transform of the pulse $d(t) - d_0(t)$ for a chain length of 101 spins with a total time $T = 56.50J^{-1}$.

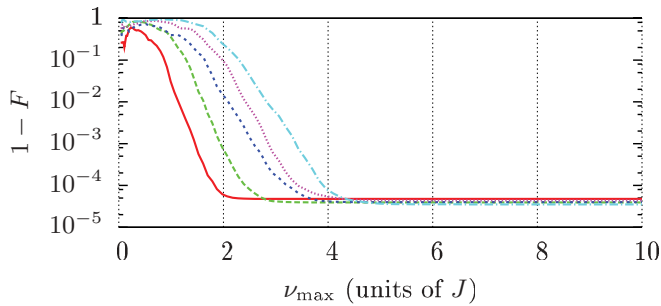


FIG. 12. (Color online) The infidelity of the transfer related to the maximum frequency component of the controls retained after filtering. For key, see Fig. 10.

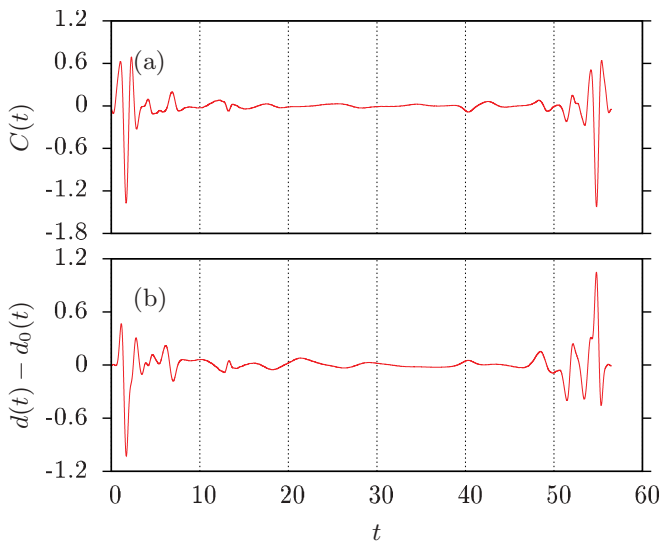


FIG. 13. (Color online) The optimal control pulses for (a) $C(t)$ and (b) $d(t) - d_0(t)$, where $d_0(t) = 1.77t$. The maximum frequency component is $\sim 4J$.

IV. THEORETICAL LIMITS OF NONRELATIVISTIC QUANTUM THEORY

Does the limit T_{QSL}^* discussed in the last chapter have a physical origin, or is it simply a numerical constraint, stemming from the construction of the optimization routine itself? If, in fact, we *are* able to reach the physical limit by application of optimal control routines, then it would appear that optimal control cannot only be used to improve the operation of experimental implementations, but indeed to probe a system's dynamics and physical limits. This connection was already investigated in Ref. [29]; here, we elucidate further the methods that were applied and draw more specific conclusions.

The physical limits on quantum systems (and hence any physical system) have been investigated theoretically in quantum systems for several years; such considerations led Lloyd in [28] to calculate the maximum rate at which any machine can process information [28]. In particular, the notion of a “quantum speed limit” has been reported by several authors. We briefly recount this theory and its particular application to our problem.

A. The quantum speed limit

What is the absolute maximum speed at which we can transfer information along our chain? This amounts to finding the minimum time it takes for the given initial state $|\Psi(0)\rangle$ to evolve to the goal state $|\varphi_N\rangle$. A possible route for finding this minimum time was explored by Carlini *et al.* [30], where it was shown that one may derive the time-optimal Hamiltonian for a given state evolution by minimizing the quantum action S of the system, by which the problem may be interpreted as a quantum analog of the classical brachistochrone. In principle, the same procedure could be performed in our case, but the complexity of the calculation is prohibitive for a many-body system like ours. Hence, we ask a more general question, as in Giovannetti *et al.* [26]: how fast can a quantum system under a time-independent Hamiltonian evolve in time?

The notions of energy and time are not inseparable, an idea that presents itself in the enigmatic time-energy uncertainty relation [40]. Hence, the minimum time in which we can perform some given evolution must be connected to the related energy scales. This minimum time is referred to as the quantum speed limit. For the case where the evolution is from an initial state to an orthogonal state for a time-independent Hamiltonian, this relation can be written explicitly as [26]

$$\tau_{\text{QSL}} \equiv \max \left(\frac{\pi \hbar}{2E}, \frac{\pi \hbar}{2\Delta E} \right), \quad (14)$$

with

$$\Delta E \equiv \sqrt{\langle \psi(0) | [\hat{H} - E]^2 | \psi(0) \rangle}, \quad (15)$$

$$E \equiv \langle \psi(0) | \hat{H} | \psi(0) \rangle. \quad (16)$$

As pointed out, this is only valid when the time evolution is governed by a time-independent Hamiltonian: E and ΔE are a measure of the energy resources available in the system only at the initial time, which for time-independent Hamiltonians defines a fixed energy scale. In our case, the methodology must be slightly modified, by considering instead the *mean* energy

spread of our system as it evolves under our time-dependent Hamiltonian, which we find by averaging the instantaneous energy spread of the system over the time interval $[0, T]$. By integrating over time, we effectively apply the bound to infinitesimal time steps dt where the Hamiltonian is approximately constant. We modify the definition in Eq. (14) to read [29]

$$\tau_{\text{QSL}} \equiv \max \left\{ \frac{\pi \hbar}{2J}, \frac{\pi \hbar}{2\Delta\mathcal{E}_2} \right\}, \quad (17)$$

where

$$\Delta\mathcal{E} = \frac{1}{T} \int_0^T \Delta E(t) dt, \quad (18)$$

with

$$\Delta E(t) \equiv \sqrt{\langle \Psi(t) | [\hat{H}(t) - E(t)]^2 | \Psi(t) \rangle}, \quad (19)$$

$$E(t) \equiv \langle \Psi(t) | \hat{H}(t) | \Psi(t) \rangle. \quad (20)$$

As was already pointed out, this speed limit defines the time it takes to rotate from the initial state to an orthogonal state. Since the initial and final sites are not directly coupled, we cannot immediately rotate from the initial state to our goal state. Due to this condition, we postulate that the speed limit must be interpreted as an effective *time-per-site*; the total time it takes to traverse the chain is this time-per-site multiplied by the number of sites (minus one) in the chain, or equivalently, the number of edges we have between the initial state vertex and the final state vertex when one views the spin chain as a connected graph.

Equation (17) effectively states that the minimum time it takes to rotate from the current system state to an orthogonal state is bounded from below by $\pi\hbar/(2J)$ [we shall see later that for the evolutions we consider, the second term in Eq. (17) is always less than this term, so that we can neglect it]. By considering the speed limit of a simple two-spin system with a coupling strength J , we can associate this bound with the time it takes to swap an excitation between only two sites, given that for the initial state the excitation is completely localized on one of the two sites. Using the reasoning above, we see that the quantum speed limit theory predicts that the minimum time to traverse the chain is given simply by the time it takes to perform a swap between two neighboring sites (which we shall henceforth refer to as “orthogonal swaps”) multiplied by the number of sites in the chain (minus one). However, in our particular system, at some intermediate time it may be (as we have already seen from the results in Sec. III) that the excitation does not perform repeated swap operations, but rather moves along the chain as a dispersed “wave.” If one now imagines the picture of the excitation wave moving from site to site, we note that two excitation waves centered at neighboring sites are not orthogonal, unlike when we have the excitation fully localized on a single site. This means that we can expect the actual propagation time to be *shorter* than the one calculated from simply doing repeated orthogonal swap operations. The optimized system performs a controlled excitation-wave propagation, which we can view as a cascade of *effective* swap operations, each shorter in duration than that

given by the orthogonal swap. We are then motivated to write the total time to traverse the chain as

$$T_{\text{QSL}} = \gamma(N - 1)\tau_{\text{QSL}}, \quad (21)$$

where γ is a dimensionless constant that quantifies the effective swap duration in terms of the orthogonal swap. As a side remark, we note that one can also imagine mapping the full chain with the effective swaps onto a shorter chain with orthogonal swaps, which is analogous to a reduction of the transmission length of the chain. Similar ideas have already been explored for long-range interactions in Ref. [41].

B. Comparing limits

As already alluded to in Sec. III there comes a point where the optimal control algorithm is no longer able to reach an optimal solution. We aim to show that this limit on the evolution time (which we denoted by T_{QSL}^*) corresponds to the quantum speed limit for the system T_{QSL} discussed in Sec. IV A.

The procedure for determining T_{QSL}^* is as follows. We select a chain length N , and set some initial evolution time T which we assume to be longer than the corresponding T_{QSL}^* . We perform optimal control on the system for a fixed number of iterations R . We then repeat this for shorter and shorter times T . The results of the simulations are shown in Fig. 14. Note that we plot the effective time-per-site $(T - b)/(N - 1)$ in order to make comparisons between chains of differing lengths easier. One sees clearly that for longer times, we are able to complete the state transfers with high fidelities. As we reduce the time, we begin to see that the final value of the infidelity does not converge to zero, even after many thousands of iterations of the control algorithm. Somewhere in between these two extremes lies the limit of the optimal control algorithm. We quantify this by setting a threshold ε for the infidelity; the time T_{QSL}^* for each N is defined as the smallest value of the time T for which the infidelity $I < \varepsilon$ after R iterations. This threshold obeys a linear relation:

$$T_{\text{QSL}}^* \approx a(N - 1) + b,$$

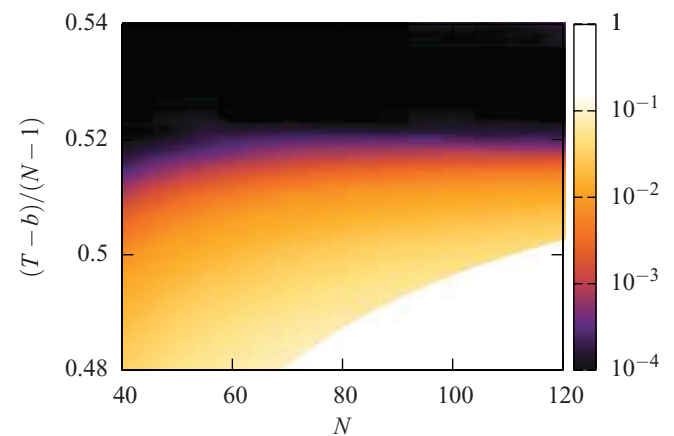


FIG. 14. (Color online) The infidelity reached after $R = 100,000$ iterations for different chain lengths N and effective time-per-site $(T - b)/(N - 1)$, where $b = 3.65$.

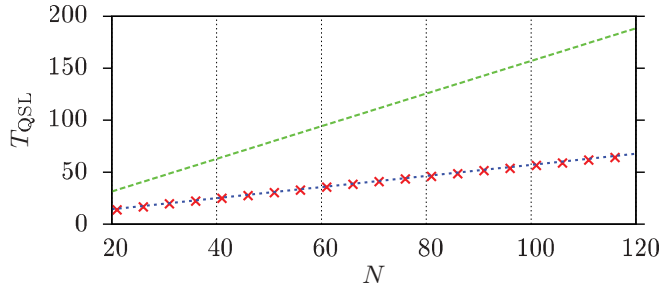


FIG. 15. (Color online) A comparison of the quantum-speed-limit time T_{QSL} with the optimal control limit T_{QSL}^* . The solid (red) line is T_{QSL} with $\gamma = 1$, which is the repeated orthogonal swaps. The (blue) crosses are T_{QSL}^* for different N in the range 21–131 with $\varepsilon = 5 \cdot 10^{-5}$. The dashed (green) line is $T_{\text{QSL}} + b$ with $\gamma = 0.34$.

with $a = 0.34$ and $b = 3.65$. Note that this is *a posteriori* the same b used in the effective time-per-site $(T - b)/(N - 1)$ for Fig. 14. The introduction of the constant b describes additional effects due to the boundaries of the chain, where the excitation wave is generated at the beginning of the evolution, and then collapsed into a localized excitation at the end. Additionally, b is not dependent on N (unless the chain length is of the order of the width of the spin wave).

We now compare the results from the quantum speed limit T_{QSL} with T_{QSL}^* , which is shown in Fig. 15. In order to evaluate Eq. (17) for each value of N , we must numerically calculate the second term in the bracket, since it depends upon the time-evolved state $|\psi(t)\rangle$. For all points at our defined threshold, this comes out to be less than the first term in the bracket in Eq. (17), so that the speed limit is given simply by the effective swap time. One finds that optimal control outperforms what can be achieved through applying repeated swap operations between adjacent spins. Furthermore, by ignoring boundary effects for T_{QSL}^* , we find that our model for the quantum speed limit fits the data with a value of $\gamma = 0.34$. This means that the speed limit achieved with the optimal control can be described (ignoring the ends of the chain) as a cascade of effective swaps.

V. CONCLUSION

We have shown that we can successfully apply optimal control to the system given in Eq. (2) to produce fast

transfers of excitations along spin chains; two orders of magnitude faster, in fact, than was reported in Ref. [1] for comparable fidelities. This has application in the fast transport of quantum states over short distances. Furthermore, we have found a fundamental limit for optimal control beyond which optimization is not possible, and identified it as a speed limit on the dynamics of the system, which is manifested by the dynamics as the propagation of an excitation wave with constant velocity. We compare this with the standard formulation of the quantum speed limit, and show that for our many-body problem, the quantum speed limit implies that the optimal strategy for transport is characterized by effective swaps along the chain. We confirm this through a comparison with the numerical results.

It is interesting to note that aside from the theory on the quantum speed limit, there is a large body of work concerned with a similar bound specifically for spin systems, namely the Lieb-Robinson bound [42–44]. It would be interesting to investigate the connection between this bound and the QSL (which will be the subject of future research), although it is likely difficult to quantify this explicitly.

We have shown that not only is optimal control a useful tool for the optimization of tasks relevant for quantum information processing (specifically transmission of quantum information along a spin chain), but also as a means to probe the limits of many-body quantum systems where the theoretical methods become unwieldy. We expect that given the generality of the method, it should be able to probe fundamental limits of many quantum systems that can be efficiently simulated. Indeed, we used the same technique to prove a bound on the duration of a unitary SWAP operation on a spin chain, showing that it was achievable in a time that scaled only polynomially with the number of sites [8] (although it was not shown that this was a fundamental limit). We will continue with such investigations in future work.

ACKNOWLEDGMENTS

We thank L. Viola for valuable discussions. We acknowledge financial support by the European Union under the contracts MRTN-CT-2006-035369 (EMALI), IP-EUROSQP, IP-SCALA, and IP-AQUTE, and from the German SFB TRR21. We thank the bwGRID for computational resources.

-
- [1] V. Balachandran and J. Gong, *Phys. Rev. A* **77**, 012303 (2008).
 - [2] S. Bose, *Contemp. Phys.* **48**, 13 (2007).
 - [3] O. Romero Isart, K. Eckert, and A. Sanpera, *Phys. Rev. A* **75**, 050303(R) (2007).
 - [4] M. Christandl, N. Datta, A. Ekert, and A. J. Landahl, *Phys. Rev. Lett.* **92**, 187902 (2004).
 - [5] V. Subrahmanyam, *Phys. Rev. A* **69**, 034304 (2004).
 - [6] S. Bose, *Phys. Rev. Lett.* **91**, 207901 (2003).
 - [7] A. Kay, *Phys. Rev. A* **73**, 032306 (2006).
 - [8] D. Burgarth, K. Maruyama, M. Murphy, S. Montangero, T. Calarco, F. Nori, and M. B. Plenio, *Phys. Rev. A* **81**, 040303(R) (2010).
 - [9] D. Burgarth, V. Giovannetti, and S. Bose, *Phys. Rev. A* **75**, 062327 (2007).
 - [10] V. Giovannetti and D. Burgarth, *Phys. Rev. Lett.* **96**, 030501 (2006).
 - [11] T. Calarco, U. Dörner, P. S. Julienne, C. J. Williams, and P. Zoller, *Phys. Rev. A* **70**, 012306 (2004).
 - [12] S. Montangero, T. Calarco, and R. Fazio, *Phys. Rev. Lett.* **99**, 170501 (2007).
 - [13] G. De Chiara, T. Calarco, M. Anderlini, S. Montangero, P. J. Lee, B. L. Brown, W. D. Phillips, and J. V. Porto, *Phys. Rev. A* **77**, 052333 (2008).
 - [14] T. Schulte-Herbrüggen, A. Spörl, N. Khaneja, and S. J. Glaser, *Phys. Rev. A* **72**, 042331 (2005).

- [15] N. Khaneja, T. Reiss, C. Kehlet, T. Schulte-Herbrüggen, and S. J. Glaser, *J. Magn. Reson.* **172**, 296 (2005).
- [16] M. Grace, C. Brif, H. Rabitz, I. A. Walmsley, R. L. Kosut, and D. A. Lidar, *J. Phys. B* **40**, S103 (2007).
- [17] V. Nebendahl, H. Häffner, and C. F. Roos, *Phys. Rev. A* **79**, 012312 (2009).
- [18] A. Spörl, T. Schulte-Herbrüggen, S. J. Glaser, V. Bergholm, M. J. Storz, J. Ferber, and F. K. Wilhelm, *Phys. Rev. A* **75**, 012302 (2007).
- [19] S. Schirmer, *J. Mod. Opt.* **56**, 831 (2009).
- [20] R. Nigmatullin and S. G. Schirmer, *New J. Phys.* **11**, 105032 (2009).
- [21] C. M. Tesch and R. de Vivie-Riedle, *Phys. Rev. Lett.* **89**, 157901 (2002).
- [22] S. E. Sklarz and D. J. Tannor, *Phys. Rev. A* **66**, 053619 (2002).
- [23] D. J. Tannor, V. A. Kazakov, and V. Orlov, in *Time-Dependent Quantum Molecular Dynamics*, edited by J. Broeckhove and L. Lathouwers (Plenum Press, New York, 1992), pp. 347–360; J. Somloi, V. A. Kazakov, and D. J. Tannor, *Chem. Phys.* **172**, 85 (1993); J. P. Palao and R. Kosloff, *Phys. Rev. Lett.* **89**, 188301 (2002); *Phys. Rev. A* **68**, 062308 (2003).
- [24] S. G. Schirmer and P. J. Pemberton-Ross, *Phys. Rev. A* **80**, 030301(R) (2009).
- [25] M.-H. Yung, *Phys. Rev. A* **74**, 030303(R) (2006).
- [26] V. Giovannetti, S. Lloyd, and L. Maccone, *Phys. Rev. A* **67**, 052109 (2003); *J. Opt. B* **6**, S807 (2004).
- [27] P. Pfeifer, *Phys. Rev. Lett.* **70**, 3365 (1993).
- [28] S. Lloyd, *Nature (London)* **406**, 1047 (2000).
- [29] T. Caneva, M. Murphy, T. Calarco, R. Fazio, S. Montangero, V. Giovannetti, and G. E. Santoro, *Phys. Rev. Lett.* **103**, 240501 (2009).
- [30] A. Carlini, A. Hosoya, T. Koike, and Y. Okudaira, *Phys. Rev. Lett.* **96**, 060503 (2006); *Phys. Rev. A* **75**, 042308 (2007).
- [31] N. Khaneja, R. Brockett, and S. J. Glaser, *Phys. Rev. A* **63**, 032308 (2001).
- [32] N. Khaneja, S. J. Glaser, and R. Brockett, *Phys. Rev. A* **65**, 032301 (2002).
- [33] T. O. Reiss, N. Khaneja, and S. J. Glaser, *J. Magn. Reson.* **165**, 95 (2003).
- [34] R. Fisher, H. Yuan, A. Spörl, and S. Glaser, *Phys. Rev. A* **79**, 042304 (2009).
- [35] D. Burgarth and S. Bose, *New J. Phys.* **7**, 135 (2005).
- [36] D. Burgarth and S. Bose, *Phys. Rev. A* **71**, 052315 (2005).
- [37] D. Burgarth, V. Giovannetti, and S. Bose, *J. Phys. A* **38**, 6793 (2005).
- [38] J. Crank and P. Nicolson, *Adv. Comput. Math.* **6**, 207 (1996).
- [39] L. B. Levitin and T. Toffoli, “The fundamental limit on the rate of quantum dynamics: the unified bound is tight,” (2009), e-print [arXiv:0905.3417](https://arxiv.org/abs/0905.3417).
- [40] P. Busch, *Time in Quantum Mechanics* (Springer, New York, 2008), Chap. 3.
- [41] G. Gualdi, V. Kostak, I. Marzoli, and P. Tombesi, *Phys. Rev. A* **78**, 022325 (2008).
- [42] E. H. Lieb and D. W. Robinson, *Commun. Math. Phys.* **28**, 251 (1972); D. W. Robinson, *The ANZIAM Journal* **19**, 387 (1976).
- [43] S. Bravyi, M. B. Hastings, and F. Verstraete, *Phys. Rev. Lett.* **97**, 050401 (2006).
- [44] A. Hamma, F. Markopoulou, I. Prémont-Schwarz, and S. Severini, *Phys. Rev. Lett.* **102**, 017204 (2009).